http://dx.doi.org/10.5935/0103-5053.20150256

J. Braz. Chem. Soc., Vol. 27, No. 1, 109-118, 2016.
Printed in Brazil - ©2016 Sociedade Brasileira de Química
0103 - 5053 $6.00+0.00

Article

Semi-Empirical Quantum Chemistry Method for Pre-Polymerization Rational Design of Ciprofloxacin Imprinted Polymer and Adsorption Studies

Luiz D. Marestoni,[a,b] Ademar Wong,[a] Gustavo T. Feliciano,[a] Mary R. R. Marchi,[a] César R. T. Tarley[,c] and Maria D. P. T. Sotomayor[a]*

[a]*Instituto de Química, Universidade Estadual Paulista "Júlio de Mesquita Filho", 14800-900 Araraquara-SP, Brazil*

[b]*Instituto Federal do Paraná, 84269-090 Telêmaco Borba-PR, Brazil*

[c]*Departamento de Química, Universidade Estadual de Londrina, 86050-482 Londrina-PR, Brazil*

It is well known that selectivity of molecularly imprinted polymers (MIPs) depends on adequate choice of functional monomer before the experimental synthesis. Computational simulation seems to be an ideal way to produce selective MIPs. In this work, we have proposed the use of semi-empirical simulation to obtain the best monomer able to strongly interact with ciprofloxacin. Twenty functional monomers were evaluated through semi-empirical quantum chemistry method and three MIPs were synthesized using the monomers acrylamide (M5), acrylic acid (M4) and 1-vinylimidazole (M16), yielding the maximum adsorption capacities of 282.0, 223.8 and 202.5 μmol g^{-1}, respectively, as predicted by the computational simulation. From competitive adsorption studies in the presence of structurally similar compounds, the MIP synthesized with acrylamide was found to possess higher specific selectivity factors (S) if compared to non-imprinted polymer (NIP), thus indicating good recognition selectivity for the ciprofloxacin.

Keywords: molecularly imprinted polymers, antibiotic, adsorption isotherm

Introduction

Ciprofloxacin (CIP) is an antibiotic that belongs to the second-generation of the fluoroquinolone chemical group. It has been used for the prophylaxis and treatment of diseases of the skin, urinary tract, respiratory tract and gastrointestinal infections. The drug can also be used as food additives for mass gain promotion.[1] Similarly to other antibiotics, CIP can cause serious side effects to human health, including nausea, vomiting, diarrhea and dizziness as well as the emergence and spread of drug-resistant bacterial strains and the possible induction of cancer.[2] Ciprofloxacin is excreted from the body via urine and feces, in which more than 75% is unmetabolized. Bearing in mind its side effects to human health, concerns about drug residues entering the food chain and/or potable water and contributing to bacterial resistance has been increasingly evidenced, mainly if one considers the increase of world population, agricultural practices and food production.[3,4] The presence of antibiotics residues in groundwater, tap water and surface water has already been reported, which justifies the growing interest in developing new and efficient procedures for treatment of water containing pollutants.[5-7] Processes based on adsorption are certainly considered to be the most effective, inexpensive and simplest for the removal of pollutants from aqueous media in comparison to chemical precipitation and electrolysis.[8-10] Indeed, the availability of a wide range of commercial adsorbents when associated to required properties for solid phase extraction, including high surface area, quick adsorption kinetics, high adsorption capacity and high reusability, make the solid phase extraction extremely attractive for the removal of organic pollutants from aquatic environments.[11] However, the selectivity also plays an important role in adsorption processes, which is extremely dependent on the chemical nature of the adsorbent. In this sense, MIPs have attracted considerable attention over the past decade for the development of more selective adsorption processeses.[12] MIPs are artificially synthesized macromolecular materials in the presence of template molecules, which establish specific interactions with functional monomers. After polymerization and further removal of template from

*e-mail: ctarleyquim@yahoo.com.br

the polymeric matrix, the resulting material will leave cavities complementary in shape and size of the target molecule.[13] As has been well documented in literature,[14-17] the selectivity of MIPs depends on adequate choice of the functional monomer and, in this sense, the most common approach for attaining this task is through the synthesis of several MIPs with different monomers. Obviously, this approach is considered to be expensive and time-consuming, which justifies the use of computational simulation to overcome these drawbacks. Computational simulation makes possible to quantify and predict the properties that describe the binding process. Thus, it has been considered a very interesting tool for choosing the most suitable materials for the adsorption process, saving time and chemical resources.[18-23]

Some published studies with focus on the application of MIPs for CIP determination in food (milk, egg and chicken), urine and water samples have been reported.[24-28] However, most of them refer to the application of MIP as adsorbent in complex matrices, but a theoretical study through computational simulation approach, as well as important competitive adsorption studies for assessing the selectivity of MIPs and adsorption isotherm studies, are still few exploited.

According to the aforementioned, this work deals with semi-empirical quantum chemistry approach to study twenty pre-polymerization reaction possibilities for CIP. In order to check the efficiency of computational simulation as an outstanding tool for MIPs preparation, especially in choosing the adequate monomers, three MIPs with different monomers were synthesized and compared among them regarding the selectivity and adsorption capacity. The polymers were also characterized through scanning electron microscopy (SEM) and textural data.

Experimental

Chemical structure of molecules

Geometry optimizations and energy calculations were performed to determine the best interaction between CIP and those monomers commonly cited in literature for MIP preparation. The monomers are shown in Table 1 and were named as M1 to M20.

The chemical structure of CIP is shown in Figure 1.

To optimize the choice of the best monomer, the computer simulation was carried out with six interfering molecules: norfloxacin (NOR), nalidixic acid (NAL), amoxicillin (AMX), tetracycline hydrochloride (TCL), chloramphenicol (CLR) and uric acid (URC), which chemical structures are also shown in Figure 1.

Table 1. Monomers used for semi-empirical quantum chemistry and their chemical structures

Symbol	Monomer	Chemical structure
M1	*N*,*N*'-methylenebisacrylamide	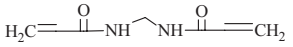
M2	imidazole-4-acrylic acid	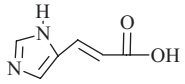
M3	imidazole-4-acrylic ethylester	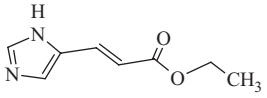
M4	acrylic acid (AA)	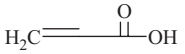
M5	acrylamide (ACL)	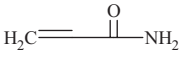
M6	acrolein	
M7	allylamine	
M8	acrylonitrile	
M9	ethylene glycol dimethacrylate	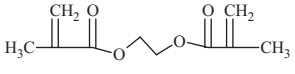
M10	2-aminoethyl methacrylate	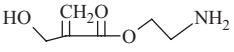
M11	methylene succinic acid	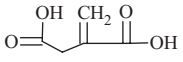
M12	methacrylic acid	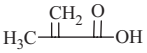
M13	1,3-divinyl-benzene	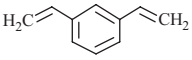
M14	1,4-divinylbenzene	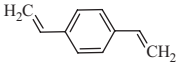
M15	styrene	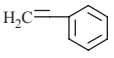
M16	1-vinylimidazole (1-VN)	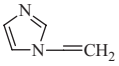
M17	2-vinylpyridine	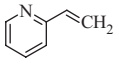
M18	4-vinylpyridine	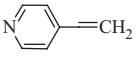
M19	2-acrylamido-2-methyl-1-propanesulfonic acid	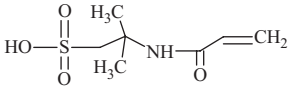
M20	2-hydroxyethyl methacrylate	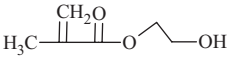

Platform and software

The simulation was performed using a desktop PC running Microsoft Windows XP Professional operating

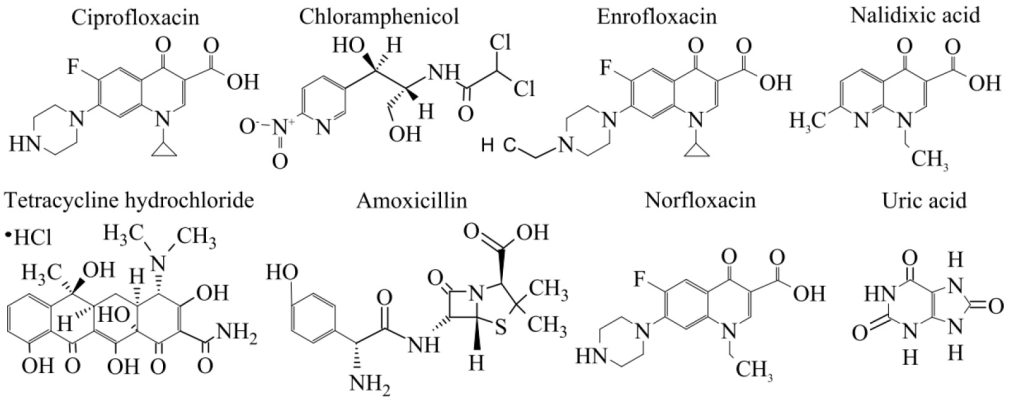

Figure 1. Chemical structure of ciprofloxacin.

system (Microsoft Corp., Redmond, Washington, USA), configured with a 1.6 GHz Pentium Dual-Core (Intel, Santa Clara, California, USA), CPU 2140 processor having 4 GBytes of double data rate type three synchronous dynamic random-access memory (RAM DDR3).

The molecules were generated and minimized using the program HyperChem 8.0.5 (Hypercube, Inc., Gainesville, Florida, USA). The software package OpenEye (under academic license, OpenEye Scientific Software, Inc., Santa Fe, New Mexico, USA) was used for simulations, which contain: VIDA 3.0.0, that allowed to check possible errors in the bonds between atoms, post calculation analysis and representation; OMEGA2, that generate conformers of molecules; and SZYBKI 1.2.2, which provides more stability for the molecule.

The entire process was scripted, automated and executed using Autolt 3.3.6.0, a freeware BASIC-like scripting language, which uses the scripts to automate repetitive processes during modeling, and MMH with Mopac2009,[29] a semi-empirical quantum chemistry program based on Dewar and Thiel's neglect of diatomic differential overlap (NDDO) approximation with parameterization method 6 (PM6) using experimental and *ab initio* data. This program simulates the association-free energies (E) interaction *in vacuo*, according to equation 1.

$$E = E_{AB} - (E_A + E_B) \quad (1)$$

where E_{AB} represents the total energy of a system containing one molecule and one CIP molecule, subtracting the free energy of each molecule individually one with energy E_A, and one monomer molecule with energy E_B.[30]

Computational design

Before simulation, the structure of the selected molecules were initially optimized using molecular mechanics assisted model building and energy refinement (AMBER) force field, with the steepest descents algorithms converging at 0.1 kJ mol^{-1} in 720 as maximum cycles, designed in zwitterion mode and saved as program database (PDB) file containing information about their composition and atoms positions.

All molecules were energy minimized using SZYBKI (OpenEye Scientific Software, Inc., Santa Fe, New Mexico, USA), and OMEGA (OpenEye Scientific Software, Inc., New Mexico, USA) was used to obtain possible stable conformers to take into account molecule flexibility. The resulting set of conformers for TPL and monomers was saved in an office saved search (OSS) format file containing information about partial charges assigned to each atom and their spatial coordinates. Then the molecules were analyzed by MMH using two kinds of minimization keywords: the former am1 efmmok t = 3d xyz, for minimizing every single molecule by the semi-empirical quantum chemistry method before calculating the complex interaction; and the latter am1 efmmok t = 3d geo-ok int, used for minimizing every single cell of the complex ligand-target.[31]

The parameters chosen in the MMH program were: number of random structure cells, in this case, 100; the binding energies values of hydrogen bonds, aromatic, electrostatic, hydrophobic, van der Waals forces, and dipole–dipole interactions, were obtained up to a maximum distance of 4 Å from any molecule; the temperature was kept at 298 K and the convergence energy at 0.001 kJ mol^{-1}. Once the run completed, a file with all summarized statistical results together with the molecule files containing the docked structures was generated. Computation times, thermodynamic properties, association energies (E_{AB}, kJ mol^{-1}), and association-free energies (E, kJ mol^{-1}) were taken as the main results to study the binding of the complex ligand-target.

From the result of the interaction of CIP with twenty functional monomers designed in Table 1, the monomers

which gave the highest ratio CIP/interfering molecule of the binding score, smallest score and intermediate score were selected for the polymer preparation. The main driving force that we observed for the binding was the electrostatic interaction between the molecules, especially regarding the dipole moment and the hydrogen bond. In this sense, the C–N group of the M8 compound (acrylonitrile) displayed both properties at the same time, which explains the largest interaction energies observed for all molecules related to CIP.

Syntheses of MIPs

All syntheses were performed within a 25 mL thick-walled glass tube, in which 0.1 mmol of CIP (≥ 98.0%, Fluka, St. Gallen, Switzerland), 0.4 mmol of monomer chosen after simulation, 3.2 mmol of ethylene glycol dimethacrylate (EDGMA) and 0.1 mmol of azobisisobutyronitrile (AIBN; all monomers and reagents from Sigma-Aldrich, St. Louis, Missouri, USA) were dissolved in 7.0 mL of acetonitrile (high-performance liquid chromatography grade, J.T. Baker Chemical Company, Phillipsburg, New Jersey, USA). The mixture was sonicated for 5 min and degassed with nitrogen for 10 min. The tube was sealed with plastic film and considering that CIP decomposes under UV irradiation, thermal polymerization was chosen in this work, at 60 °C for 24 h.

The resulting polymer was ground in a mortar. The particle size was controlled by passing the polymer through an 80 mesh sieve. The polymer was washed using a Soxhlet extractor with a mixture of methanol and acetic acid (9:1, v/v) to remove the CIP from polymeric matrix. The solvent was replaced daily and analyzed. The washing step was finished when CIP was no longer quantified in the solvent. Non-imprinted polymer (NIP) were prepared similarly, without CIP, and treated identically. All polymers were dried at 70 °C and kept in this condition prior to use.

Characterization of MIPs

The textural data were determined for the three MIPs synthesized with acrylic acid (M4), acrylamide (M5) and 1-vinylimidazole (M16). The average pore sizes of the polymers were estimated by the Barrett-Joyner-Halenda (BJH) method, based on nitrogen sorption experiments using a Quantachrome Nova 1200e automatic instrument (Boynton Beach, Florida, USA). The specific surface areas were determined from sorption isotherms according to the Brunauer-Emmett-Teller (BET) method. Prior to the analyses, the polymers were dried at 80 °C for 6 h.

Scanning electron microscopy images were determined only for the polymer synthesized with the acrylic acid due to its better adsorption property towards the CIP. A SEM using a FEI Quanta 200 (Phillips, Amsterdam, North Holland, The Netherlands) at an accelerating voltage of 30 kV was used for obtaining the images. Prior to the analyses, the polymer was coated with a thin layer of gold-palladium alloy, using a Bal-Tec MED 020 equipment, in order to minimize charging under the incident electron beam.

Adsorption studies

Batch rebinding experiments were carried out at 298 K ± 1% by adding 50 mg of MIP or NIP in contact with 5.0 mL of different concentrations of CIP, ranging from 0.1 to 2 mmol L^{-1}, under pH 3.5 in acetonitrile-water (50:50, v/v) medium. The mixture was stirred during 120 min and centrifuged for 10 min at 4000 rpm. The supernatant was filtered with a membrane of 0.45 μm (Millipore, Merck, Darmstadt, Hesse, Germany) and analyzed by high-performance liquid chromatography (HPLC). The maximum adsorption capacity (M) was calculated to evaluate the binding properties of the MIP. The adsorption experiments data were further adjusted using Freundlich (FR), Langmuir (LA), Redlich-Peterson (RP), Langmuir-Freundlich (LF), Dubinin-Raduskevich (DR), Toth (TO) and Temkin (TK) models.[32,33]

Competitive adsorption experiments were performed for assessing the selectivity of MIP towards the CIP in comparison to NIP. The experiments were performed in the same experimental conditions of the batch rebinding experiments. Binary solution containing CIP and structurally similar compounds (NOR, NAL, AMX, TCL, CLR or URC) were stirred with MIP or NIP. Firstly, the adsorbate partition coefficient (K_p, mL g^{-1}) was determined according to equation 2:[34]

$$K_p = \frac{Q}{C} \quad (2)$$

where Q is the concentration of compounds *per* gram of polymer (mg g^{-1}) and C is the final concentration of compounds in the supernatant (mg mL^{-1}). The selectivity of one molecule *vs.* another is called separation factor (α). This is defined in the equation 3 and correspond to the ratio of the two partition coefficients $K_{P(CIP)}$ and $K_{P(INT)}$ for ciprofloxacin and interfering (INT) compounds, in the MIP or NIP, respectively.[34]

$$_{CIP.INT} = \frac{K_{P(CIP)}}{K_{P(INT)}} \quad (3)$$

In order to compare the imprinting effects of compounds to the distribution coefficient countered for each compound,

the imprinting factor (I) was determined as described by equation 4.

$$I = \left(\frac{K_{P(MIP)}}{K_{P(NIP)}} \right) \quad (4)$$

From the obtained imprinting factor, the specific selectivity factor (S) for the MIP in regard to NIP was calculated by equation 5.[35] This equation allows a real estimation of the imprinting effect on the selectivity.

$$S = \left(\frac{I_1}{I_2} \right) = \frac{\text{CIP. INT}_{\text{MIP}}}{\text{CIP. INT}_{\text{NIP}}} \quad (5)$$

HPLC analysis

Concentrations of CIP were determined using a Pro Star HPLC chromatographic system (Varian, Palo Alto, California, USA) equipped with a ternary pump model 230, fluorescence detector model 360 and an auto sampler with an automated injection system model 400. The sample was analyzed on Luna C18 column (5 μm, 250 × 4.60 mm) from Phenomenex (Torrance, California, USA). The chromatographic separation was based on literature data,[35] using isocratic elution with a solution of 0.02 mol L^{-1} H_3PO_4 and acetonitrile (80:20, v/v) at a flow rate of 1.2 mL min^{-1}. The excitation and emission wavelengths were 280 and 480 nm, respectively. Standard solutions to obtain the external calibration curve were prepared by dilution in the mobile phase, obtaining final concentrations ranging from 0.01 to 1 mg L^{-1}.

Results and Discussion

Molecular modeling

The free energy of association between molecules and the monomer was calculated *in vacuo* as shown in Figure 2.

The monomer M8 (acrylonitrile) has been the most suitable for synthesis of the MIP for CIP due to its high free energy. Despite this finding, this monomer was not chosen for the MIP synthesis due to its better interaction with the other interfering compounds, mainly the uric acid. This behavior is in agreement with those previously published.[36] The monomer M9 (ethylene glycol dimethacrylate) was considered to be the one that showed the lowest free energy of association with CIP. Thus, this monomer was not chosen for the synthesis either. The results herein obtained were somewhat expected, since the monomers containing electronegative atoms, such as nitrogen and oxygen, would favor the formation of monomer-ciprofloxacin complex, taking into account the chemical structure of CIP.

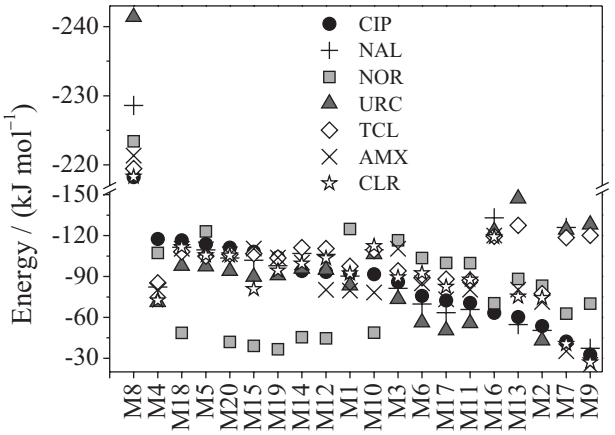

Figure 2. Results of the free energy of association of the semi-empirical quantum chemistry method for ciprofloxacin (CIP) and interfering molecules.

To validate theoretical results, three MIPs for CIP were synthesized. The monomer M4 (acrylic acid) was used, which presented the second maximum binding energy for CIP, the better ones compared with interferences; the M5 (acrylamide), that belongs to the intermediate energy region and similar free energy for CIP and interfering molecules; and M16 (1-vinylimidazole), that belongs to the minimal affinity region and lower free energy than all interfering molecules.

Characterization of MIPs

As it is well documented in literature, the adsorption process is greatly dependent on the surface area of adsorbent. Table 2 shows the values of surface area for the three MIPs and respective NIPs (M4, M5 and M16).

Table 2. Specific surface area of the polymers

Polymer	Specific surface area / (m^2 g^{-1})		
	AA[a] (M4)	ACL[b] (M5)	1-VN[c] (M16)
Molecularly imprinted polymer	392.2	382.5	380.9
Non-imprinted polymer	363.1	370.4	351.3

[a]Acrylic acid; [b]acrylamide; [c]1-vinylimidazole.

It was observed that both MIPs and NIPs showed much larger surface area in comparison to another MIPs previously synthesized for CIP. Yan *et al*.,[24] synthesized an MIP for ciprofloxacin using 2-hydroxyethyl methacrylate as monomer and methanol:water (4:1, v/v) as porogenic solvent, having a specific surface of 291 m^2 g^{-1}. The synthesis of MIPs on the surface of magnetic carbon nanotubes for CIP extraction in eggs, using methacrylic

acid as monomer and dimethyl sulfoxide (DMS) as porogenic solvent, has been reported. This material showed a specific surface area of 182.7 $m^2 g^{-1}$. The lower surface area of these previously reported materials as compared with the present study may be explained probably due to differences among the monomers and porogenic solvent used in the syntheses. In addition to these findings, MIPs showed only a slightly larger surface area with respect to the corresponding NIPs. Therefore, any differences of CIP adsorption onto MIP and NIP would not be attributed to the morphological features, but most likely due to imprinted sites created during polymer synthesis.

Figure 3 shows the SEM images of polymers synthesized with acrylic acid as monomer. As observed, both MIP and NIP revealed a rough surface with aggregated particles in the shape of microspheres. This morphological feature is of paramount importance in adsorption processes, which makes the mass transfer of molecules towards polymer surface easier and, as a consequence, adsorption capacity higher. A more detailed observation of morphological features of polymers made possible to infer that the surface of MIP and NIP is formed from irregular voids located between clusters of the microspheres (macropores > 50 nm diameter) or from the interstitial space of a given cluster of microspheres (mesopores, 2-50 nm diameter), or even within the microspheres themselves (micropores < 2 nm = 20 Å radius).[34] The latter one could correspond to the selective cavities. The presence of micropores in the MIP was confirmed from BET experiments. The obtained value was 14.91 Å, which is within the range expected to MIP pore size, as indicated in Figure 3. In order to verify whether the cavity ascribed to the micropores (14.91 Å) corresponds to the selective size of CIP molecule, a computational modeling by a quantum mechanical geometry optimization calculation, using density functional theory (DFT), was carried out to estimate the size of the molecule taking into account the electronic structure. The region defining the molecule was considered as the region where the total electronic density has a value greater than 0.00001 e $Å^{-3}$. The value of the major axis length of CIP yielded the value of 14.29 Å, being very close (difference of only 4.3%) to the experimental BET results. This result suggests that MIP synthesized with acrylic acid can be considered as a nanosize selective material, suggesting that this material can be successfully used for the extraction of trace amounts of CIP. It is worth to emphasize that using the DFT, we have herein used the Perdew-Burke-Ernzerhof parametrization of the generalized gradient approximation (GGA-PBE) exchange-correlation functional, with a polarized double-zeta basis set. The program used was SIESTA. The chosen cut-off for the electron density (10^{-5} e $Å^{-3}$) is close to the experimental uncertainty of the most sophisticated X-ray measurement techniques, and thus, it is expected to accurately describe the size of the molecule inside the cavity, and if this cut-off is further decreased, the change in the size is in the fourth digit of the molecule size, in Å.

Adsorption studies

The pH and solvent composition (expressed in $\%H_2O$ in acetonitrile) has an important role on the CIP adsorption. The pH was included in the experimental design due to pH dependence of the CIP molecule. The experimental assays for this optimization study were performed by stirring a standard solution of 0.15 mmol L^{-1} CIP in presence of 50 mg of each MIP during 60 min (Figures 4a and 4b).

As observed, the best adsorption of CIP was achieved between pH 2.0 and 3.5 using 50% of water for all MIPs

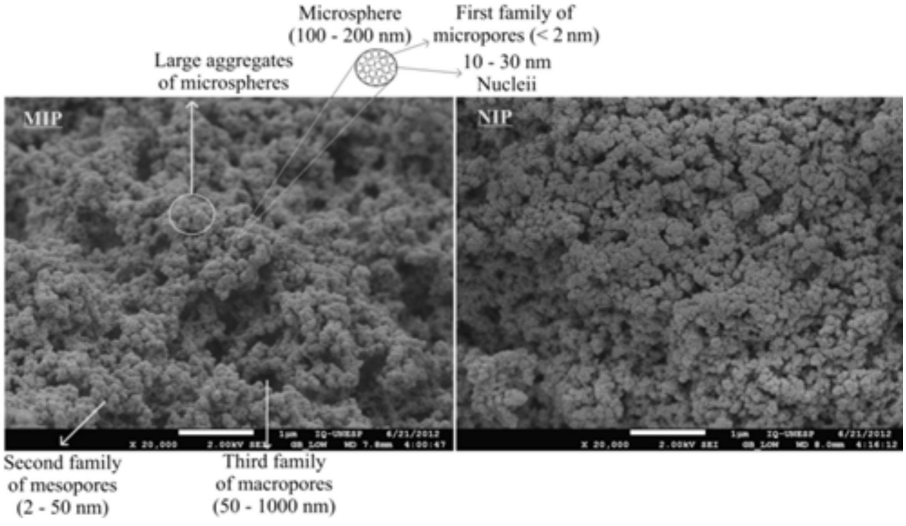

Figure 3. Scanning electron microscopy (SEM) images of molecularly imprinted polymer (MIP) and non-imprinted polymer (NIP).

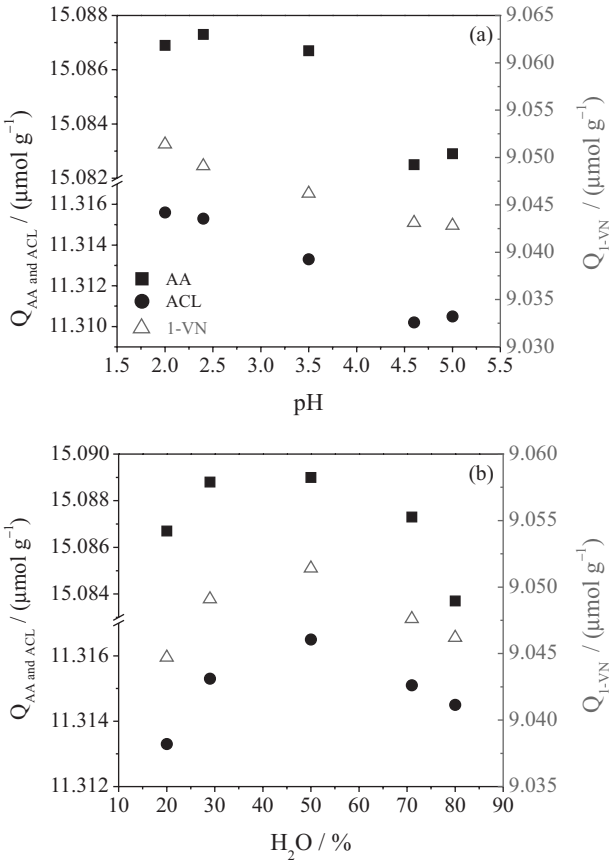

Figure 4. (a) Influence of pH and (b) solvent composition (H_2O:acetonitrile) on the adsorption of ciprofloxacin on different polymers.

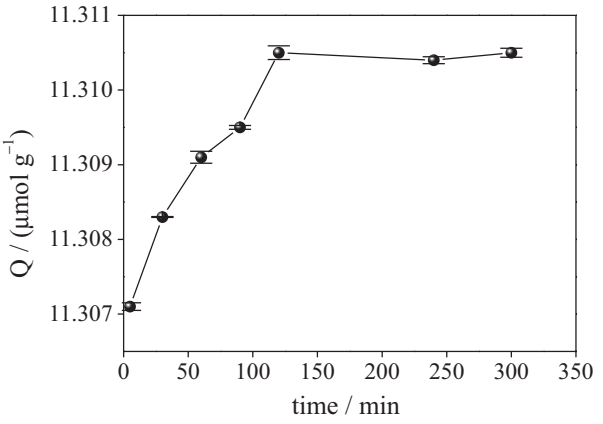

Figure 5. Influence of contact time on the adsorption profile of ciprofloxacin on molecularly imprinted polymer (MIP).

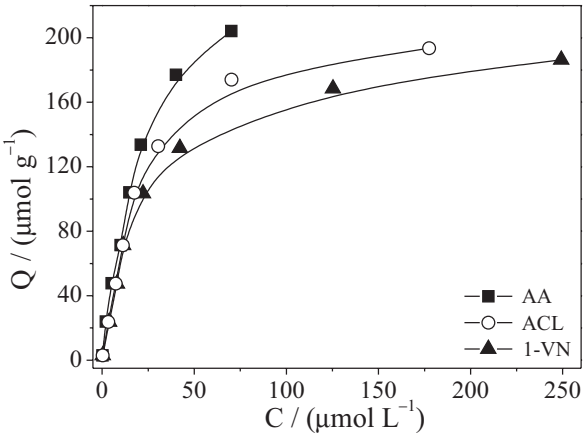

Figure 6. Experimental isotherms of molecularly imprinted polymer (MIP) synthesized with different monomers: acrylic acid (AA), acrylamide (ACL) and 1-vinylimidazole (1-VN).

investigated. Furthermore, since the MIP synthesized with acrylic acid showed the best results for adsorption of CIP, further experiments were carried out at pH 3.5 and 50% of water.

The influence of contact time on the CIP adsorption onto MIP is illustrated in Figure 5. It was clearly observed that the equilibrium time was achieved in 120 min, indicating a quick mass transfer of CPI towards the surface of MIP. Thus, for further experiments this time was used.

Isotherms of adsorption for MIP are shown in Figure 6. The equation parameters and the underlying thermodynamic assumptions of these isotherms often provide some insight into both the adsorption mechanism and the surface properties and affinity of the adsorbent.

The parameters of isotherms as well as the regression coefficient (R^2) and mean square of residuals (σ) are shown in Table 3. The FR isotherm is an empirical model that can be applied to non-ideal adsorption on heterogeneous surfaces as well as multilayer sorption. The LA isotherm is the most widely applied adsorption isotherm and predicts a constant monolayer adsorption capacity. The RP isotherm incorporates features of both the LA and FR. At low concentrations, the RP isotherm approximates to LA isotherm and at high concentrations its behavior approaches that of the FR isotherm. The derivation of the TK isotherm assumes that the decrease in temperature of adsorption is linear rather than logarithmic, as implied in the FR equation. The TO isotherm has proven useful in describing sorption in heterogeneous systems. It assumes an asymmetrical *quasi*-Gaussian energy distribution with a widened left-hand side. The LF isotherm considers the case of a molecule occupying two sites.[32,33] The equations for these isotherms are shown in Table 3.

The choice of the better isotherm model that best fits the data to determine the parameters were performed taking into account a higher R^2 and lower σ. As can be observed from Table 3, the models that presented the best adjustments were LA and LF isotherm. The similarity among them was somewhat expected, once the parameter β, which means the heterogeneity of binding sites, was very close to one for LF isotherm. Therefore, we can assume that LA adsorption model explains the adsorption of CIP onto MIP. It is worth emphasizing that the maximum adsorption capacity (M)

Table 3. Ciprofloxacin adsorption isotherm parameters for different molecularly imprinted polymer (MIP)

Model	Equation	Monomer	K^k / (L μmol^{-1})	M^l / (μmol g^{-1})	β^m	R^2	σ^n
LA[a]	$Q = \frac{KMC}{1+KC}$	AA[h]	0.0396 ± 0.0036	282 ± 11	–	0.995	24.4
		ACL[i]	0.0446 ± 0.0039	223.8 ± 7.1	–	0.993	32.3
		1-VN[j]	0.0434 ± 0.0028	202.5 ± 4.1	–	0.996	15.9
FR[b]	$Q = KC^{\beta}$	AA[h]	24.5 ± 4.5	–	0.514 ± 0.049	0.967	170.5
		ACL[i]	30.3 ± 7.7	–	0.378 ± 0.058	0.903	468.7
		1-VN[j]	29.1 ± 6.9	–	0.352 ± 0.050	0.919	363.4
LF[c]	$Q = \frac{KMC^{\beta}}{1+KC^{\beta}}$	AA[h]	0.0357 ± 0.0066	265 ± 23	1.08 ± 0.11	0.995	26.8
		ACL[i]	0.0263 ± 0.0035	204.7 ± 3.9	1.258 ± 0.058	0.998	7.1
		1-VN[j]	0.0352 ± 0.0063	195.4 ±5.7	1.102 ± 0.077	0.997	14.2
RP[d]	$Q = \frac{KMC}{1+KC^{\beta}}$	AA[h]	$(3.1 \pm 2.4) \times 10^{45}$	24.5 ± 6.7	0.486 ± 0.090	0.961	204.6
		ACL[i]	$(5.8 \pm 3.8) \times 10^{45}$	30.3 ± 9.4	0.622 ± 0.086	0.884	562.4
		1-VN[j]	$(4.6 \pm 3.1) \times 10^{46}$	29.1 ± 7.6	0.647 ± 0.056	0.903	436.1
TO[e]	$Q = \frac{KMC}{(1+KC^{\beta})^{\beta-1}}$	AA[h]	1.04 ± 0.99	$(1.37 \pm 0.26) \times 10^{-6}$	−0.03 ± 0.30	0.958	219.6
		ACL[i]	0.0066 ± 0.0036	1132 ± 570	1.52 ± 0.15	0.998	8.0
		1-VN[j]	0.026 ± 0.016	303 ± 150	1.13 ± 0.16	0.996	16.3
DR[f]	$\log Q = \log^2 (KC)^{\beta} + \log M$	AA[h]	0.0061 ± 0.0025	10.56 ± 0.42	0.057 ± 0.013	0.994	33.0
		ACL[i]	0.0065 ± 0.0006	9.831 ± 0.067	0.062 ± 0.005	0.997	13.2
		1-VN[j]	0.0041 ± 0.0008	9.61 ± 0.11	0.047 ± 0.007	0.994	28.1
TK[g]	$Q = \frac{M}{B}\ln(KC)$	AA[h]	2.0 ± 1.3	3.8 ± 1.8	0.11 ± 0.36	0.766	1219.4
		ACL[i]	1.4 ± 0.9	3.4 ± 2.0	0.099 ± 0.047	0.840	772.2
		1-VN[j]	1.2 ± 0.9	3.5 ± 1.6	0.113 ± 0.059	0.893	477.6

[a]Langmuir; [b]Freundlich; [c]Langmuir-Freundlich; [d]Redlich-Peterson; [e]Toth; [f]Dubinin-Raduskevich; [g]Temkin; [h]acrylic acid, [i]acrylamide; [j]1-vinylimidazole; [k]adsorbate-adsorbent affinity; [l]maximum adsorption capacity; [m]heterogeneity of binding sites; [n]mean square of residuals. Results are expressed as mean value ± standard deviation based on three replicates (n = 3).

obtained from the LA model for MIPs were very close to the experimental data (Figure 6), which confirms once again the best adjustment of this model to the experimental isotherm. Among the studied polymers, MIP synthesized with acrylic acid was found to possess the highest M. These findings corroborate the computational simulation, which confirms its outstanding capacity for predicting the best retention capacity of the polymer.

Selectivity

In order to evaluate the formation of selective cavities in the MIP, competitive adsorptions in batch using molecules with similar structure to the CIP were performed. The same experiments were carried out by using the NIP. A similar adsorption profile of CIP and those interfering molecules indicate the presence of undesirable cross-reactivity in the MIP. Thus, for this study, the interfering molecules of the simulation were selected. The selectivity of CIP was evaluated and the respective MIP and NIP adsorption capacities are shown in Table 4, using the equations 3, 4 and 5. As can be seen in Table 4, the obtained values for imprinting factors (I) for CIP were higher when compared with the ones achieved for structurally similar molecules, which indicates that MIP has higher molecular recognition to CIP with respect to NIP. In addition, the specific selectivity factor (S) was higher than one in all cases, as a consequence of the existence of molecular memory in the imprinted polymer with selective size (14.91 Å), tridimensional shape and specific binding interaction. The obtained S of 1.31 Å for the binary system ciprofloxacin-norfloxacin also demonstrates the good selective adsorption of CIP by the MIP even in the presence of very structurally similar molecule.

Conclusions

This study described the use of theoretical calculation for the pre-selection of a suitable functional monomer able to interact with large organic compounds, ciprofloxacin in the current study, in obtaining a highly selective molecularly imprinted polymer. In addition to the obtained

Table 4. Selectivity parameters obtained for the polymers

Polymer		C^j / (mg L^{-1})	Q^k / (μmol g^{-1})	K_p^l / (mL g^{-1})	α^m		I^n	S^o
MIP[a]	CIP[c]	8.4	4.2	166.73	6.41	CIP[c]	2.17	5.55
	AMX[d]	16.4	1.3	25.99				
NIP[b]	CIP[c]	12.2	2.8	76.96	1.16	AMX[d]	0.39	
	AMX[d]	12.9	2.6	66.57				
MIP[a]	CIP[c]	9.1	3.9	144.15	6.522	CIP[c]	1.71	5.42
	NAL[e]	16.9	1.1	22.10				
NIP[b]	CIP[c]	11.7	2.9	84.11	1.203	NAL[e]	0.32	
	NAL[e]	12.6	2.6	69.90				
MIP[a]	CIP[c]	9.3	3.9	138.25	7.723	CIP[c]	2.14	9.72
	CLR[f]	17.4	0.9	17.90				
NIP[b]	CIP[c]	13.0	2.5	64.58	0.795	CLR[f]	0.22	
	CLR[f]	11.9	2.9	81.25				
MIP[a]	CIP[c]	9.9	3.6	121.97	1.355	CIP[c]	1.03	1.31
	NOR[g]	11.4	3.1	90.01				
NIP[b]	CIP[c]	10.0	3.6	118.65	1.032	NOR[g]	0.78	
	NOR[g]	10.2	3.5	114.99				
MIP[a]	CIP[c]	8.9	3.9	146.81	8.252	CIP[c]	2.24	7.62
	TCL[h]	17.4	0.9	17.79				
NIP[b]	CIP[c]	12.9	2.5	65.55	1.082	TCL[h]	0.29	
	TCL[h]	13.3	2.4	60.56				
MIP[a]	CIP[c]	7.9	4.3	180.68	7.750	CIP[c]	2.73	9.19
	URC[i]	16.7	1.2	23.31				
NIP[b]	CIP[c]	12.9	2.6	66.08	0.844	URC[i]	0.30	
	URC[i]	12.1	2.89	78.31				

[a]Molecularly imprinted polymer; [b]non-imprinted polymer; [c]ciprofloxacin; [d]amoxicillin; [e]nalidixic acid; [f]chloramphenicol; [g]norfloxacin; [h]tetracycline hydrochloride; [i]uric acid; [j]final concentration of compounds in the supernatant concentration; [k]concentration of compounds *per* gram of polymer; [l]adsorbate partition coefficient; [m]separation factor; [n]imprinting factor; [o]specific selectivity factor.

selectivity, the MIPs synthesized showed greater surface area in comparison to other MIPs previously published in literature. The results achieved by computational are in agreement with the ones obtained by experimental adsorption data. MIP synthesized with acrylic acid was found to possess the highest adsorption and selectivity for ciprofloxacin in the presence of structurally similar compounds with respect to NIP. From the SEM images and textural data, we have also demonstrated that the high selectivity of MIP was not attributed to the morphological features. These findings show once again that the best and highest selective adsorption of CIP on the MIP synthesized with acrylic acid, as predicted by the computational simulation, depend, in fact, on the selective binding sites created during polymer synthesis. For final remarks, the theoretical calculation can be exploited for obtaining molecularly imprinted polymers, saving time and reducing the costs of synthesis.

Acknowledgements

We acknowledge the agencies Fundação de Amparo à Pesquisa do Estado de São Paulo (FAPESP), Instituto Nacional de Ciência e Tecnologia de Bioanalítica (INCTBio), Fundação Araucária - Paraná, Coordenação de Aperfeiçoamento de Pessoal de Nível Superior (CAPES), Conselho Nacional de Desenvolvimento Científico e Tecnológico (CNPq) and PRÓ-FORENSES (CAPES) by financial support.

References

1. IIo, C. E.; IIondu, N. A.; Okwoli, N.; Brown, S. A.; Elo-Ilo J. C.; Agabasi, P. U.; Orisakwe, O. E.; *Am. J. Ther.* **2006**, *13*, 432.
2. Tamim, H. M.; Musallam, K. M.; Kadri, H. M. A.; Boivin, J. F.; Collet, J. P.; *Eur. J. Obstet. Gynecol. Reprod. Biol.* **2011**, *159*, 388.

3. Oliveira, H. M. V.; Moreira, F. T. C.; Sales, M. G. F.; *Electrochim. Acta* **2011**, *56*, 2017.
4. Githinji, L. J. M.; Musey, M. K.; Ankumah, R. O.; *Water Air Soil Poll.* **2011**, *219*, 191.
5. Alvero, C. C.; *System. Appl. Microbiol.* **1994**, *9*, 169.
6. Campeau, R. C.; Gulli, L. F.; Graves, J. F.; *Microbios* **1996**, *88*, 205.
7. Yiruhan.; Wang, Q. J.; Mo, C. H.; Li, Y. W.; Gao, P.; Tai, Y. P.; Zhang, Y.; Ruan, Z. L.; Xu, J. W.; *Environ. Pollut*. **2010**, *158*, 2350.
8. Derylo-Marczewska, A.; Blachnio, M.; Marczewski, A. W.; Swiatkowski, A.; Tarasiuk, B.; *J. Therm. Anal. Calorim*. **2010**, *101*, 785.
9. Wells, M. J.; Yu, L. Z.; *J. Chromatogr. A* **2000**, *885*, 237.
10. Oliveira, T. F.; Ribeiro, E. S.; Segatelli, M. G.; Tarley, C. R. T.; *Chem. Eng. J.* **2013**, *221*, 275.
11. Tarley, C. R. T.; Kubota, L. T.; *Anal. Chim. Acta* **2005**, *548*, 11.
12. Ye, L.; Yu, Y.; Mosbach, K.; *Analyst* **2001**, *126*, 760.
13. Barros, L. A.; Pereira, L. A.; Custódio, R.; Rath, S.; *J. Braz. Chem. Soc*. **2014**, *25*, 619.
14. Lai, Y.; Xie, C.; Zhang, Z.; Lu, W.; Ding, J.; *Biomaterials* **2010**, *31*, 4809.
15. Brown, C. J.; Dastidar, S. G.; See, H. Y.; Coomber, D. W.; Ortiz-Lombardia, M.; Verma, C.; Lane, D. P.; *J. Mol. Biol.* **2010**, *395*, 871.
16. Tarley, C. R. T.; Sotomayor, M. D. T.; Kubota, L. T.; *Quim. Nova* **2005**, *6*, 1076.
17. Tarley, C. R. T.; Sotomayor, M. D. T.; Kubota, L. T.; *Quim. Nova* **2005**, *6*, 1087.
18. Mascini, M.; Sergi, M.; Monti, D.; Del Carlo, M.; Compagnone, D.; *Anal. Chem*. **2008**, *80*, 9150.
19. Mascini, M.; Macagnano, A.; Scortichini, G.; Del Carlo, M.; Diletti, G.; d'Amico, A.; Di Natale, C.; Compagnone, D.; *Sens. Actuators, B* **2005**, 111, 376.
20. Mascini, M.; Guilbaut, G. G.; Monk, I. R.; Hill, C.; Del Carlo, M.; Compagnone, D.; *Microchim. Acta* **2008**, *163*, 227.
21. Bini, A.; Mascini, M.; Turner, A. P. F.; *Biosens. Bioelectron*. **2011**, *26*, 4411.
22. Sanchez-Barragan, I.; Karim, K.; Costa-Fernandez, J. M.: Piletsky, S. A.; Sanz-Medel A.; *Sens. Actuators, B* **2007**, *123*, 798.
23. Mascini, M.; Del Carlo, M.; Compagnone, D.; Cozzain, I.; Tiscar, P. G.; Mpamhanga, B.; Chen, B.; *Anal. Lett*. **2006**, *39*, 1627.
24. Yan, H.; Row, K. H.; *Bull. Korean Chem. Soc.* **2008**, *29*, 1173.
25. Yan, H.; Row, K. H.; Yang, G.; *Talanta* **2008**, *75*, 227.
26. Priefo, A.; Schareder, S.; Bauer, C.; Moder, M.; *Anal. Chim. Acta* **2011**, *685*, 146.
27. Liu, S.; Yan, H.; Wang, M.; Wang, L.; *J. Agric. Food Chem*. **2013**, *61*, 11974.
28. Wang, J.; Dai, J.; Meng, M.; Song, Z.; Pan, J.; Yan, Y.; Li, C.; *J. Appl. Polym. Sci.* **2014**, *131*, 40310.
29. Stewart, J. J. P.; *Mopac2009; Stewart Computational Chemistry*; Colorado Springs, USA, 2008.
30. Meier, F.; Schott, B.; Riedel, D.; Mizaikoff, B.; *Anal. Chim. Acta* **2012**, *744*, 68.
31. Neri, G.; Donato, N.; d'Amico A.; Di Natale, C.; *Sensors and Microsystems,* Springer: New York, 2011.
32. Jahanshahi, M.; Panahi, H. A.; Hajizadeh, S.; Moniri, E.; *Chromatographia* **2008**, *68*, 41.
33. Ho, Y. S.; Porter, J. F.; McKay, G.; *Water Air Soil Poll.* **2002**, *141*, 1.
34. Spivak, D. A.; *Adv. Drug Delivery Rev*. **2005**, *57*, 1779.
35. Cheong, S. H.; McNiven, S.; Rachkov, K.; Levi, R.; Yano, K.; Karube, I.; *Macromolecules* **1997**, *30*, 1317.
36. Kamel, A. H.; Mahmoud, W. H.; Mostafa, M. S.; *Anal. Methods* **2011**, *3*, 957.

Submitted: May 11, 2015
Published online: October 2, 2015

FAPESP has sponsored the publication of this article.